

Optoelectronic and Photophysical Properties of Polyfluorene Blends as Side-Chain Length and Shape

Ho Yun Byun,^{†,§} In Jae Chung,^{*,†,§} Hong-Ku Shim,^{‡,§} and Chung Yup Kim[⊥]

Department of Chemical and Biomolecular Engineering, KAIST, 373-1 Guseong-dong, Yuseong-gu, Daejeon, Korea 305-701; Department of Chemistry, KAIST, 373-1 Guseong-dong, Yuseong-gu, Daejeon, Korea 305-701; Center for Advanced Functional Polymer, KAIST, 373-1 Guseong-dong, Yuseong-gu, Daejeon, Korea 305-701; and E-polymer laboratory, Samsung Advanced Institute of Technology, Suwon 449-712, Korea

Received February 3, 2004; Revised Manuscript Received May 7, 2004

ABSTRACT: The effects of side chain length and shape at the C-9 position of fluorene in poly(9,9'-dihexylfluorene) (PDHF), poly(9,9'-dioctylfluorene) (PDOF), and poly(9,9'-dicyclohexylheptylfluorene) (PDHHF) on optoelectronic and photophysical properties have been investigated in terms of Förster-type energy transfer when they are blended with poly(*N*-vinylcarbazole) (PVK). PVK/PDHF (w/w, 90/10) shows much more improved photoluminescence and electroluminescence properties than PVK/PDOF (90/10) and PVK/PDHHF (90/10). The rate (k_T) and the efficiency (E_T) of energy transfer in polymer blends which are obtained from optical properties and fluorescence intensity decay reveal that they depend on the donor–acceptor distance (r), which is altered by the side chain length of fluorene, rather than the spectral overlap integral (J). PVK/PDHHF (90/10) having polyfluorene with the long and bulky cycloheptyl hexyl side chain have a long distance between donor and acceptor with which the rate and the efficiency of energy transfer decrease. However, PVK/PDHF (90/10) shows the best optoelectronic properties due to the short side chain length of PDHF.

Introduction

π -Conjugated polymers with aromatic or heterocyclic units have been applied in electronic and optical devices such as polymer light-emitting diodes (PLEDs),¹ lasers,² photovoltaic cells,³ sensors,⁴ thin-film transistors,⁵ and photodetectors⁶ because conjugated polymers are semiconductive with band gaps in the range 1.5–3.0 eV. They are photoexcited by absorbing UV or visible light, and their electronic excitations accompanied by a change in bond length and in electronic density generate excitons (electron–hole pairs), which are bound by Coulomb interaction. By Franck–Condon transitions, excitons relax to their ground state radiatively or nonradiatively. Radiative relaxations consist of fluorescence and phosphorescence, which are spin singlet and spin triplet states, respectively.

Since soluble and processable poly(2,7-fluorene)s with attaching dialkyl substituents to the C-9 position of the fluorene core were introduced in 1989,^{7,8} poly(dialkylfluorene) (PDAF) has been widely investigated in the molecular structure of homo- and copolymer because it has a high chemical and thermal stability as well as exceptionally high fluorescence quantum yields (0.6–0.8).⁹ The alkyl side chains at the C-9 position of the fluorene unit make the polymer solution processable without changing optical and electrical properties,¹⁰ while the lower molecular weight and glass-transition temperature (T_g) are detrimental to the decay times of resulting devices. They can control the intermolecular interactions of polymers without significantly increasing

the steric hindrance in the polymer backbone. However, PDAF generally shows low-energy emission band in the range 500–600 nm besides the main emission in the solid state, regardless of bulky substitution at the C-9 position of fluorene core. The origin of the low-energy emission band has been usually attributed to aggregate and excimer formation.¹¹ The presence of keto defect (9-fluorenone) could also lead to the low-energy emission band.¹² It is known that the emission from excimer, contrary to the emission from exciton, is red-shifted and featureless, and the PL quantum yield is strongly reduced. As seen in a review paper,¹³ end-capping with monofunctional fluorene derivatives (or anthracene, or cross-linkable moieties, or hole-trapping groups) and longer side chain substitutions at the C-9 position of fluorene core are suggested to reduce the excimer emission.

Polymer–polymer blending has been practiced in the fabrication of light-emitting diodes for the following reasons.¹⁴ First, light-emitting polymers blended with an optically inert polymer such as PMMA or PS often yield a higher photoluminescence (PL) intensity on photoexcitation due to the dilution effect. Second, polymer blends between two light-emitting polymers with different band gaps often show a large enhancement in the PL intensity of the polymer with narrower band gap (acceptor) on photoexcitation of the polymer with the wider band gap (donor) by Förster energy transfer.¹⁵ The excitons created on absorption of higher energy photons at donor sites transfer the energy to acceptor molecules. This reduces the degree of exciton quenching and the excimeric emission¹⁶ and enhances the high PL and EL efficiency of donors.¹⁷ However, polymer blends are generally in a phase-separated state, one of the restrictions to have good optoelectronic properties, unless there is a strong intermolecular interaction such as hydrogen bonding or ionic attraction between the two polymers. In poorly miscible or im-

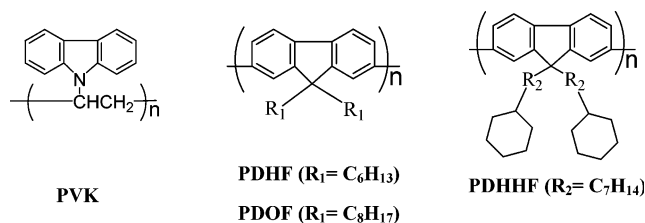
* Corresponding author: Tel +82-42-869-3916; Fax +82-42-869-3910; e-mail chung@kaist.ac.kr.

[†] Department of Chemical and Biomolecular Engineering, KAIST.

[‡] Department of Chemistry, KAIST.

[§] Center for Advanced Functional Polymer, KAIST.

[⊥] Samsung Advanced Institute of Technology.

**Figure 1.** Chemical structures of PVK and PDAF.**Table 1. Molecular Weights and Optical Properties of PVK and PDAF**

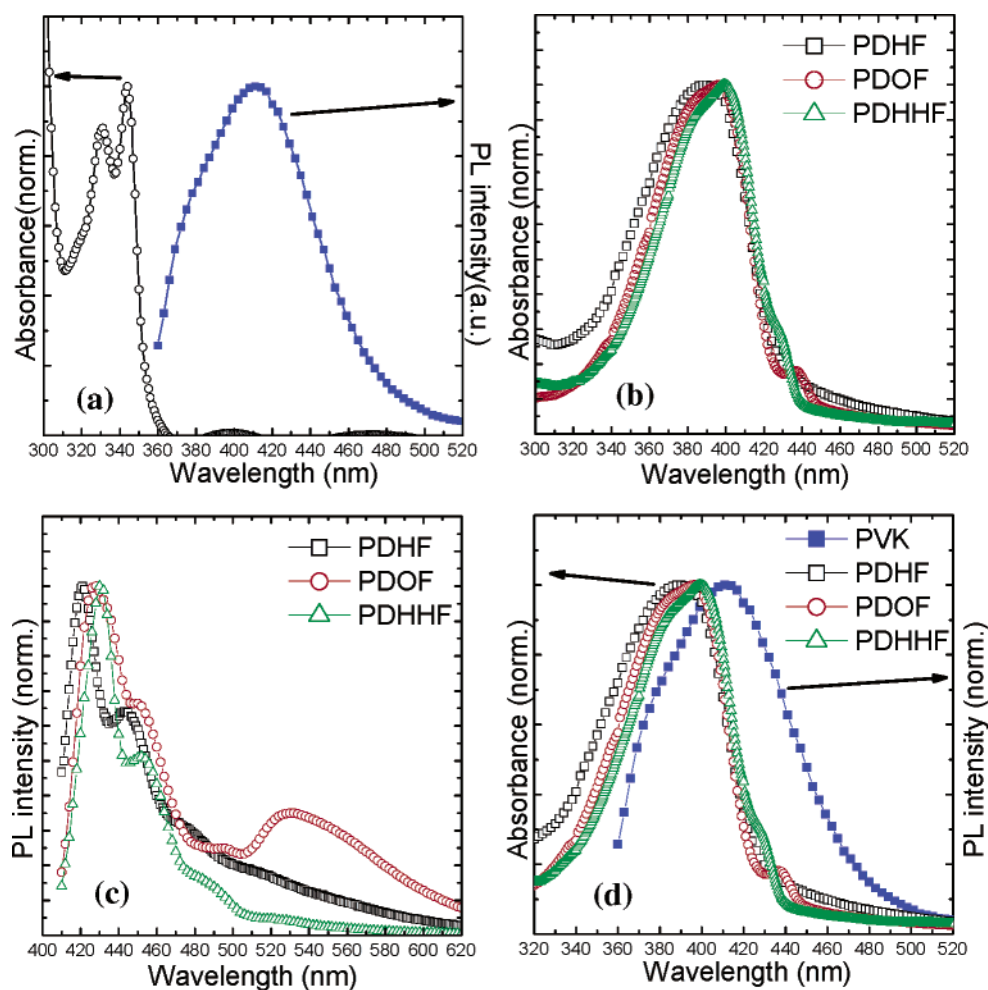
polymer	M_n	M_w	PDI	λ_{abs} (nm)	λ_{em} (nm)	optical onset (nm)
PVK		110 000		345	410	365
PDHF	7580	17 497	2.3	390	424	429
PDOF	29 347	56 059	1.9	397	430	446
PDHMF	42 700	91 900	2.1	400	429	444

miscible blends, there is a partial energy transfer between donor and acceptor within the limited interfacial region of Förster radius.¹⁸ When an exciton generated in a donor chain moves to the interface of an acceptor chain, the exciton energy is transferred to the acceptor and then decays radiatively or nonradiatively.¹⁹ So polymer/polymer interface plays an important role for the energy transfer.

There is an attempt to get a spectral stability of blue-emitting PDAF by blending with charge transport or charge blocking polymers.²⁰ The chiroptical absorption

and emission properties,²¹ thermotropic liquid crystallinity,^{22–24} and dichroic ratios²⁵ in optical properties of PDAF in an aligned thin film have been studied by its alkyl side chains.

Poly(*N*-vinylcarbazole) (PVK) is a good hole transporting material in organic light-emitting diodes,²⁶ while its quantum efficiency as an emitting layer is rather low, and light-emitting polymer blends with PVK give higher PL quantum efficiency than a homopolymer.²⁷ In this study, the optoelectronic and photophysical properties of PVK/PDAF blends have been investigated by changing the side chain length and shape of PDAF. PVK has been used as a donor material due to a higher energy band gap and a hole transporting layer because its HOMO (highest occupied molecular orbital) level, about 5.36 eV,²⁸ is between those of poly(3,4-ethylenedioxythiophene)/poly(styrenesulfonate) (PEDOT/PSS, ca. 5.2 eV)²⁹ and PDAF (ca. 5.5–5.9 eV).¹³ As alluded to above, optoelectronic properties of PDAF have been known to be unaffected by its alkyl side chain because its position is far from the conjugation. Therefore, there have been few studies on the roles of the side chain length and shape of PDAF in emissive polymer blends. Spectral overlaps between the emission of PVK and the absorption of PDAF could induce Förster-type energy transfer in their own blends. We have investigated optoelectronic and photophysical properties of the blends by changing the side chain of PDAF, and the rate and efficiency of energy transfer. EL properties are also discussed.

**Figure 2.** (a) UV-vis and PL spectrum of PVK, (b) UV-vis and (c) PL spectra of PDAF, and (d) spectral overlap between the emission of PVK and the absorptions of PDAF.

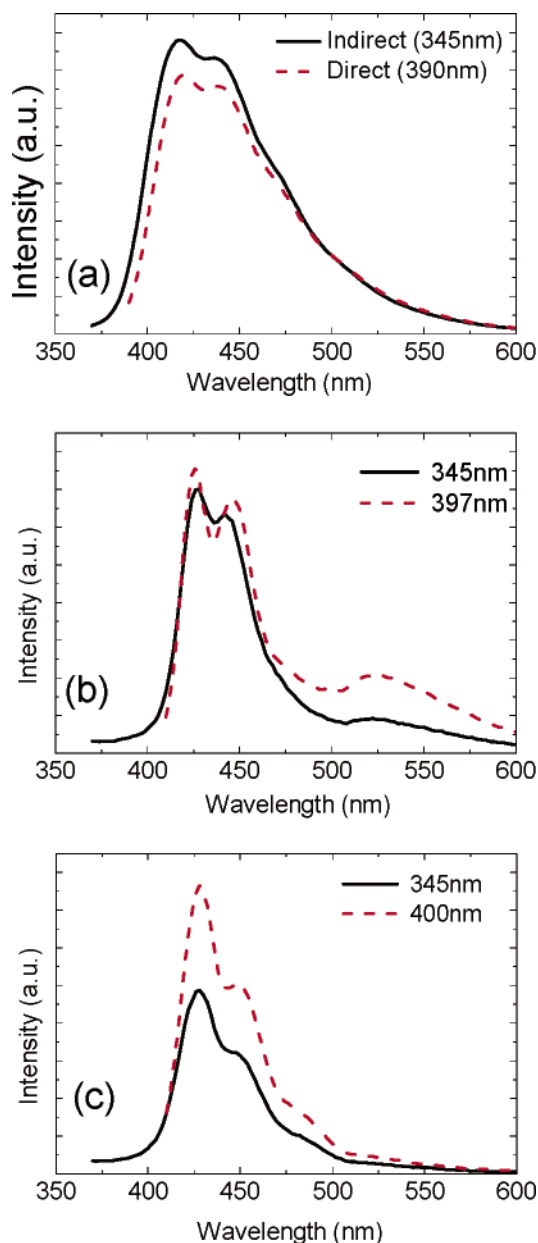


Figure 3. PL spectra of (a) PVK/PDHF (90/10), (b) PVK/PDOF (90/10), and (c) PVK/PDHHF (90/10) on indirect (—, 345 nm) or direct (---, 390–400 nm) photoexcitation. Indirect involves energy transfer while direct involves only excitation of PDAF.

Experimental Section

Materials. Poly(*N*-vinylcarbazole) (PVK) with molecular weight (M_w) of 1.1×10^6 g/mol was purchased from Aldrich. Poly(9,9-dihexylfluorene) (PDHF), poly(9,9-dioctylfluorene) (PDOF), and poly(9,9-di(cyclohexylheptyl)fluorene) (PDHHF) were synthesized by the Yamamoto coupling reaction.^{30,31}

Characterization. Polymers were identified by ^1H and ^{13}C NMR (FT 500 MHz NMR spectrometer (Bruker AMX 500)). Molecular weights of the polymers were determined by gel permeation chromatography (GPC) on a Waters WISP 712 instrument calibrated with polystyrene as the standard and THF as the eluent. UV-vis spectra were recorded on a Jasco V-530 at room temperature using a 10 mm quartz cell and solute concentration of 1×10^{-5} mol/L in chloroform in the case of solution. The films for UV-vis spectra were prepared by dissolving the polymers in chloroform and spin-coating on quartz plates. PL spectra were recorded on an ISS PC1 spectrofluorometer. The polymer solution concentrations for the PL were less than 1×10^{-5} mol/L to avoid any inner filter

effects. Thin films for the PL spectra were casted by spin-coating from a chloroform solution containing 1–2 wt % of polymers or polymer blends. Photoluminescence excitation (PLE) measurements were performed from 250 to 400 nm, monitoring the maximum intensity of emission of each sample on the same ISS PC1 spectrofluorometer. The morphology of blends was investigated by using the scanning probe microscopy (SPM, DI NanoScope IIIa). SPM measurement was performed in air with etched silicon probe, of which the length was 125 μm , and the spring constant was from 20 to 100 N/m. Scanning was carried out in the tapping mode, and its frequency was about 0.5 Hz. The time-correlated single-photon counting (TCSPC) technique was employed for the time-resolved fluorescence decay time measurements. The excitation source is a self-mode-locked picosecond Ti:sapphire laser (Coherent Co.) pumped by a Nd:YVO4 laser. Laser output has ~ 3 ps pulse width, and it spans the excitation wavelength in the ranges 235–300 and 350–490 nm by using nonlinear optical crystals. The instrument response function was measured by detecting the scattered laser pulse of about 1 ps with a quartz crystal. The resultant full width at half-maximum (fwhm) is 60 ps. This method allows a time resolution of about 20 ps after deconvolution. EL properties were characterized using a current/voltage source measurement unit (Keithley 236) and a light meter (LS-100). EL spectra were measured using an ISS PC1 spectrofluorometer.

LED Fabrication.³² Polymer light-emitting devices (PLED) of polymer blends were fabricated as follows: Poly-(3,4-ethylenedioxythiophene)/poly(styrenesulfonate) (PEDOT/PSS, Bayer Co.) solution, filtered through 0.4 μm filters (Millipore Co.), was spin-cast onto cleaned ITO glass (anode, 30 Ω , Samsung Corning Co.) and a dried 60 nm thick film at 150 $^\circ\text{C}$ for 1 h. The solutions of polymer blends (0.5–1.0 wt % in chloroform) were filtered through 0.2 μm filters (Millipore Co.) and were spin-cast onto PEDOT/PSS-coated ITO substrates. The polymer films as emitting layer were typically 60–70 nm thick. An aluminum (Al) cathode of 150 nm thickness was evaporated onto the polymer film at about 1×10^{-6} Torr.

Results and Discussion

Optical Properties of Polymers. The chemical structures of PVK and PDAF are illustrated in Figure 1. Alkyl side chain groups and bulky cyclohexyl alkyl side chain groups are introduced to decrease the intermolecular interaction in polymer chains and to increase polymer solubility.³¹ Molecular weight and optical properties of PVK and PDAF are listed in Table 1. The maximum absorption and emission peaks of PVK thin film are 345 and 410 nm, as shown in Figure 2a. In Figure 2b, the absorption spectra for thin films of PDAF are broad due to local interactions between chromophores. Disorder in molecular solids consisting of identical chromophore groups causes inhomogeneous broadening of the optical transitions of the chromophore.³³ The maximum absorption peak of PDHF is at 390 nm, which is blue-shifted about 10 nm relative to those of the others. The small molecular weight ($M_w = 17\,497$) of PDHF may be related with short conjugation length and blue-shifted absorption maximum.^{12,31} The optical onset wavelength of PDHF at 429 nm in the absorption spectrum is also blue-shifted from those of the others at 444–446 nm. Small shoulders at around 430–440 nm in the absorption spectra of PDOF and PDHHF may result from the aggregation of chains. In Figure 2c, PL spectra, corresponding to the 0–0 transition, of PDHF, PDOF, and PDHHF are in the regions of 424, 430, and 429 nm with the appearance of well-resolved vibronic peaks at 450 and 480 nm. The additional broad and featureless emission peak at 500–600 nm, which corresponds to an excimeric emission,^{34–35} appears in PDOF. It was reported that PDOF showed

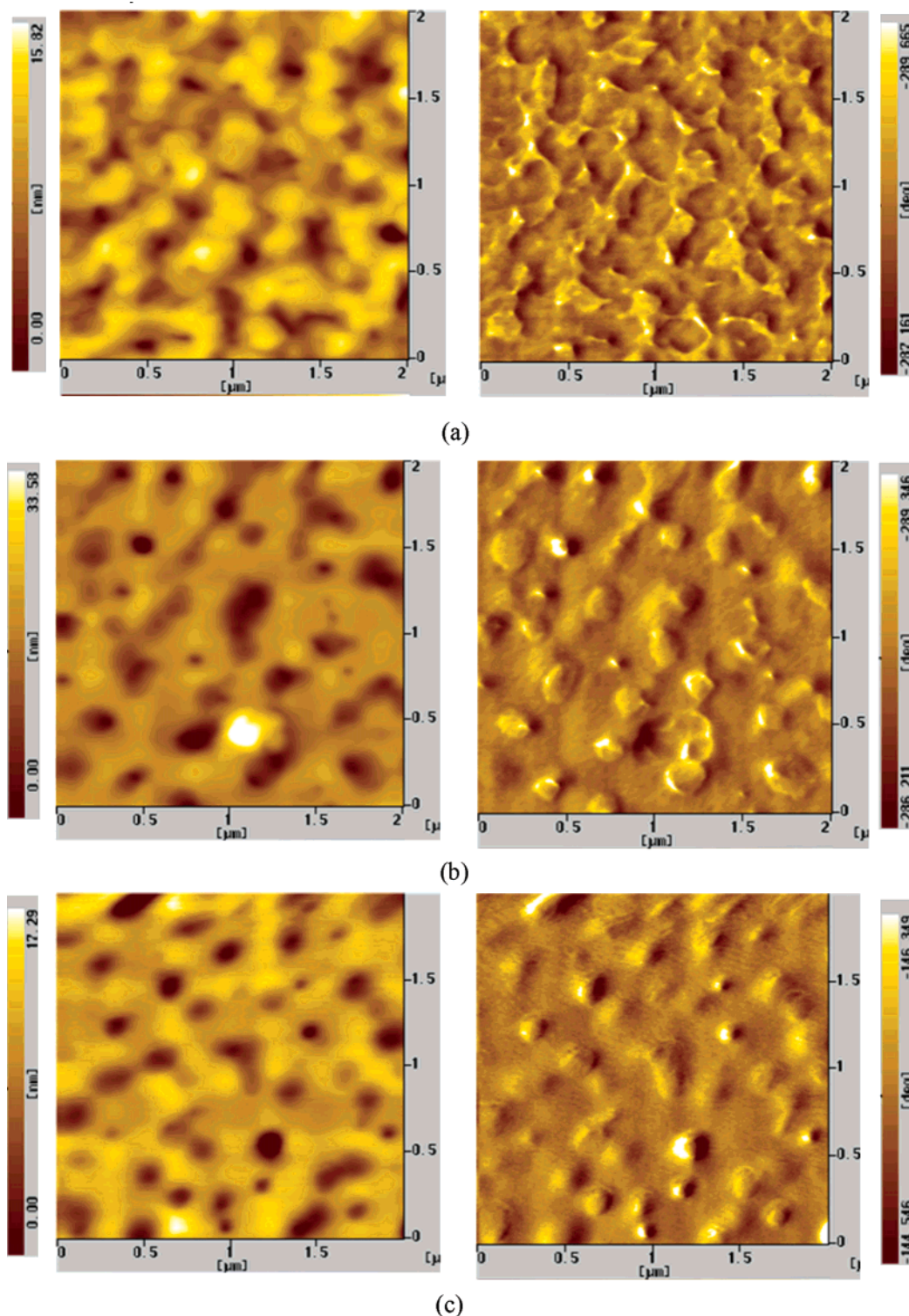


Figure 4. Tapping-mode topographical AFM images ($2 \times 2 \mu\text{m}$) of (a) PVK/PDHF (90/10), (b) PVK/PDOF (90/10), and (c) PVK/PDHHF (90/10) spin-coated from a chloroform solution. Left: height image; right: phase image.

an increase in the interchain interaction by ordering octyl side chain each other to cause the excimeric emission.¹² PDHHF has not an excimeric emission because the interaction between chains may be interrupted by its bulky cyclohexyl group at the end of long heptyl side chain, which prevents from ordering of linear alkyl chain. Considering PDHF, it is difficult to assign a broad peak around 525 nm as an excimeric emission because it could be deconvoluted from under a large vibronic band.

From the results above, the long alkyl side chain enhances the interaction between chains, which leads to a more planar extended excited state.²² However, if a bulky cyclohexyl group is introduced at the end of the long alkyl side chain, molecular interaction may be much suppressed.

Optical Properties of Polymer Blends. To investigate the effect of side chain group at the C-9 position of the fluorene unit on the PL spectrum in polymer blends, we choose PVK as a donor polymer because it

has a higher energy band gap (ca. 3.4 eV) than PDAF (ca. 2.9 eV), and its emission peak at around 410 nm is spectrally well overlapped with the absorbance of PDAF as seen in Figure 2d. Spectral overlap is one of the essential conditions to transfer exciton energy from PVK to PDAF by Förster-type energy transfer. The donor/acceptor blend ratio, PVK/PDAF (90/10, w/w), is selected by comparing the PL intensities of polymer blends. As the concentration of PDAF increases from 10 to 50 wt %, the PL intensities of the blends decrease due to phase-separated morphology and exciton quenching. It may be described that the reduction in emission of polymer blends at high concentration of PDAF is due to intermolecular interactions between PDAF chains, which lead to new nonradiative decay channels possibly involving excimer, as described in previous reports.^{36,37}

The PL spectra of PVK/PDAF (90/10) films on quartz are shown in Figure 3. When it is directly photoexcited at the absorption maximum of PDAF (390–400 nm) in the blends, which means only PDAF domains are photoexcited, the peak position of maximum emission at the 0–0 transition of PDAF is unchanged, and the broad and featureless excimeric emission¹⁶ is somewhat suppressed in PVK/PDAF (90/10) due to the dilution effect of PDAF³⁸ and the reduced amounts of interchain orders between PDAF chains in PVK. However, it is somewhat suppressed when PVK/PDOF is directly photoexcited. The interactions in PDOF domain may not be fully broken although the long side chain of PDOF. Tapping mode topographical AFM images of PVK/PDAF (90/10) blends thin films on glass substrate are shown in Figure 4. From these data, the effects of phase-separated morphology on optoelectronic and photo-physical properties are excluded because the entire polymer blends containing 10 wt % contents of PDAF show nanophase-separated morphology,³⁹ and there were no difference in morphologies.

When it is indirectly photoexcited at the absorption maximum of PVK (345 nm) in the blends, Förster-type energy transfer from PVK (a donor) to PDAF (an acceptor) occurs because the emission spectrum of PVK is spectrally overlapped with the absorption spectrum of PDAF. The PL intensity of PVK/PDHF is the most improved by efficient energy transfer (Figure 3a). In the case of PVK/PDOF, the PL intensity is slightly suppressed, and excimeric emission at around 500–600 nm is much suppressed (Figure 3b). The suppression of excimeric emission could be explained both by dilution effects of PDOF and by the rate of energy transfer.⁴⁰ Among them, the PL intensity of PVK/PDHHF decreases much (Figure 3c). To find out which chromophores contribute the emission of polymer blends, photoluminescence excitation (PLE) spectra of polymer blends were recorded with the emission monochromator centered on PDAF emission and normalized at 382 nm, as shown in Figure 5. The PLE intensity ratios at 345 nm (PVK) to that at 382 nm (PDAF) on the excitation spectrum are obtained and compared. The ratios are 1.53 (PVK/PDHF), 0.57 (PVK/PDOF), and 0.50 (PVK/PDHHF). As the ratios are large, the excitation peak of a donor (PVK) is dominant in PLE spectra, which means that PVK contribute dominantly to the emission of blends by efficient energy transfer. Therefore, energy transfer occurs more efficiently in PVK/PDHF than the others. As the side chain length of PDAF is longer, energy transfer from PVK to PDAF may be retarded in PL and PLE spectra.

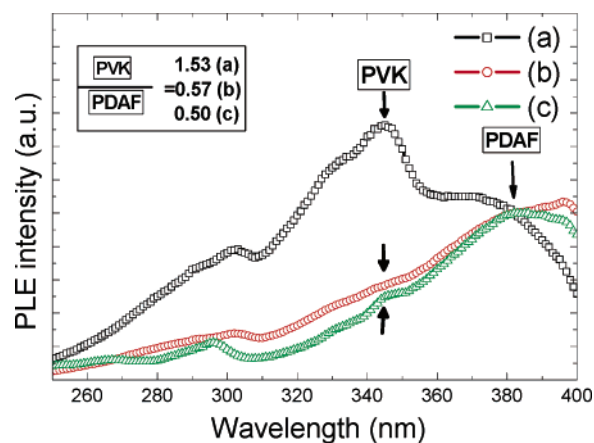


Figure 5. Photoluminescence excitation (PLE) spectra of (a) PVK/PDHF (90/10), (b) PVK/PDOF (90/10), and (c) PVK/PDHHF (90/10) normalized at 382 nm. The emission monochromator is centered on PDAF emission in polymer blends.

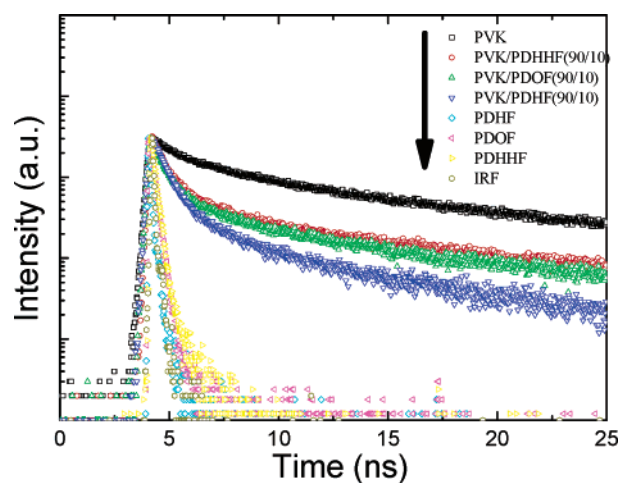


Figure 6. Time-resolved fluorescence intensity decays of PVK, PDAF, and PVK/PDAF (90/10). The excitation and fluorescence wavelength of PDAF were 377 and 425 nm. The excitation wavelengths of PVK and PVK/PDHF (90/10) were 291 nm, and their fluorescence wavelengths were 410 and 425 nm. All samples were made of thin films.

Time-Resolved Fluorescence Intensity Decay of Polymer Blends. Ultrafast spectroscopy is a particularly powerful tool for the study of energy transfer in organic materials.⁴¹ Time-resolved fluorescence decay time of PVK, PDAF, and blends are obtained by pumping at 291 nm and probing at 425 nm with the TCSPC method, as shown in Figure 6 and listed in Table 2. The decay time (τ_D) of donor (PVK) in the absence of acceptor (PDAF) which are probed at 425 nm is 12.32 ns, and the decay times of the acceptors PDAF are 168 ps (PDHF), 220 ps (PDOF), and 256 ps (PDHHF). In the polymer blends, multiexponential fluorescence decay times are found. The decay times are 4.55 ns (PVK/PDHF), 8.44 ns (PVK/PDOF), and 9.69 ns (PVK/PDHHF) when they are pumped at 291 nm and probed at 425 nm, and the decay times (τ_{DA}) of donor (PVK) in the presence of acceptor (PDAF) are 7.87 ns (PVK/PDHF), 10.82 ns (PVK/PDOF), and 11.99 ns (PVK/PDHHF). The amount of fast component, 400–600 ps, which is associated with the decay time of PDAF, decreases from 46% of decay time to 20% while the amount of slower components, 4–12 ns which are associated with the decay time of PVK, increases from 54% to 80% as the side chain length of PDAF becomes

Table 2. Time-Resolved Fluorescence Intensity Decay of Polymer and Polymer Blends^a

polymers and blends	$\lambda_{\text{exc}}/\lambda_{\text{em}}^b$ (nm)	$\tau(\text{ns})/(\alpha)^c$		τ_{avg}^e (ns) ^e
		τ_{PDAF}	τ_{PVK}	
PVK	291/425		2.10/(0.14), 13.92/(0.86)	12.32 ^f
PDHF	377/425	0.08/(0.71), 0.25/(0.27), 1.89/(0.02)		0.17
PDOF	377/425	0.20/(0.98), 1.24/(0.02)		0.22
PDHMF	377/425	0.18/(0.91), 0.64/(0.08), 3.87/(0.01)		0.26
PVK/PDHF (90/10)	291/425	0.58/(0.46)	2.62/(0.22), 11.5/(0.32) $\tau_{\text{DA}}^d = 7.87(0.54)$	4.55
PVK/PDOF (90/10)	291/425	0.46/(0.23)	2.33/(0.21), 14.00/(0.56) $\tau_{\text{DA}} = 10.82(0.77)$	8.44
PVK/PDHMF (90/10)	291/425	0.46/(0.20)	2.25/(0.20), 15.24/(0.60) $\tau_{\text{DA}} = 11.99(0.80)$	9.69

^a The excitation and fluorescence wavelengths of PDAF were 377 and 425 nm. The excitation wavelengths of PVK and PVK/PDHF (90/10) were 291 nm, and their fluorescence wavelengths were 410 and 425 nm. All samples were made of thin films. ^b $\lambda_{\text{exc}}/\lambda_{\text{em}}$ is excitation/emission wavelength. ^c τ and α are decay time and decay time fraction. τ_{PDAF} and τ_{PVK} are the decay time of PDAF and PVK. ^d τ_{DA} is the decay time of the donor, PVK, in the presence of acceptor. ^e Average decay time, τ_{avg} (ns), is calculated from $\sum \tau_i \alpha_i$. ^f τ_{D} , the decay time of donor, PVK, in the absence of acceptor. χ^2 is in the range 0.7–1.5.

longer. When efficient energy transfer occurs in the polymer blend, the amount of donor fraction in decay time should be decreased. As a result, when PVK is blended with PDAF, the energy transfer efficiency is decreased as the side chain length of PDAF becomes longer. It could be explained that the long and bulky side chain of PDHMF may fold the fluorene units to prevent PVK from approaching PDHMF and to reduce the dipole–dipole interactions, which are a requisite for Förster-type energy transfer. It is reported the large side chains of BCHA–PPV increases the host–guest spacing and hinders the Förster transfer.⁴²

Excitation energy from a donor could be transferred to an acceptor through a donor–acceptor interface. If a short-lived donor is combined with a long-lived acceptor, the exciton energy formed in a donor bulk could radiatively or nonradiatively decay in a donor bulk before it migrates to the donor–acceptor interface at which energy transfer occurs. As a result, only small fractions of exciton energy which form initially at the donor–acceptor interface will be involved in energy transfer at the interface, resulting in the lower efficiency of energy transfer. However, the fluorescence intensity decay time of PVK is about 50 times longer than that of PDAF, which is a very good condition to transfer energy.

Rate and Efficiency of Energy Transfer of Polymer Blends.⁴³ The rate of energy transfer from a donor to an acceptor (k_T) is given by

$$k_T = \frac{1}{\tau_D} \left[\frac{R_0}{r} \right]^6 \quad (1)$$

where τ_D is the decay time of the donor in the absence of acceptor, R_0 is the Förster distance, and r is the donor–acceptor distance. The expression for the Förster distance (R_0) and the overlap integral (J) is given by

$$R_0^6 = \frac{9000(\ln 10)\kappa^2 Q_D}{128\pi^5 N n^4} J$$

$$J = \int_0^\infty F_D(\lambda) e_A(\lambda) \lambda^4 d\lambda \quad (2)$$

where Q_D is the quantum yield of the donor in the absence of acceptor, n is the refractive index of the medium, N is Avogadro's number, $F_D(\lambda)$ is the corrected fluorescence intensity of the donor in the wavelength (nm) range from λ to $\lambda + d\lambda$, with the total intensity

(area under the curve) normalized to unity, $\epsilon_A(\lambda)$ is the extinction coefficient of the acceptor at λ (nm), which is typically in units of $\text{M}^{-1} \text{cm}^{-1}$, and κ^2 is a factor describing the orientation of the transition dipoles of a donor relative to that of an acceptor. It is usually assumed to be equal to $2/3$, the dynamic random average of the donors and acceptors.^{17,43} It is noticed that the transfer rate is related to the energy transfer efficiency. The energy transfer efficiency becomes much higher if the transfer rate is faster than the donor decay rate ($1/\tau_D$), while the slower transfer rate will result in inefficient energy transfer. The efficiency of energy transfer (E_T) could be represented as the fraction of photons absorbed by the donor that are transferred to the acceptor.

$$E_T = \frac{k_T}{\tau_D^{-1} + k_T} = \frac{R_0^6}{R_0^6 + r^6} = \frac{\left(\frac{R_0}{r}\right)^6}{\left(\frac{R_0}{r}\right)^6 + 1} \quad (3)$$

From eq 3, the efficiency of energy transfer is strongly dependent on the ratio of Förster distance (R_0) to the donor–acceptor distance (r). For example, when R_0 is equal to the r , the efficiency is 0.5. The efficiency decreases as r becomes larger above R_0 while it approaches 1.0 as r becomes much smaller than R_0 . It is known that R_0 is proportional to the overlap integral (J) as seen in eq 2. Therefore, as the overlap integral (J) increases, the rate (k_T) and the efficiency (E_T) of energy transfer could increase at a fixed r ^{44,45} when the orientation factor is assumed to be equal. However, different behaviors of the overlap integral (J) dependence on E_T (or k_T) are observed in PVK/PDAF blends. The overlap integral (J) of PVK/PDHMF is 1.53 times larger than that of PVK/PDHF, as listed in Table 3. Hence, it is expected that the former has the higher rate (k_T) and efficiency (E_T) of energy transfer than the latter. However, the PL intensity of PVK/PDHMF at indirect photoexcitation is decreased though it has the larger overlap integral (J) than the other blends, while PVK/PDHF having the smallest the overlap integral (J) shows the most improved PL intensity, as shown in Figure 3. Förster radii (R_0) of polymer blends are in the range 63–68 Å, as seen in Table 3. The small difference (~ 1.5 times) of overlap integral (J) does not much affect the Förster radius (R_0) in eq 2 because R_0^6 is proportional to J . It means that the donor–acceptor distance

Table 3. Spectral Overlap Integral (J), Förster Radius (R_0), Efficiency of Energy Transfer (E_T), Rate of Energy Transfer (k_T), Donor–Acceptor Distance (r) of Polymer Blends, and Length (L) of Fully Extended Alkyl Side Chains of PDAF

polymer blends	overlap integral (J)	R_0^a (Å)	E_T^b	r^c (Å)	L^d (Å)	k_T^e	
						$1/\tau_D (R_0/r)^6$	$1/\tau_D (R_0/L)^6$
PVK/PDHF(90/10)	2.21×10^{15} (1.00) ^f	63.0 (1.00)	0.36 (1.00)	69 (1.00)	7.6 (1.00)	0.047 (1.00)	26,336 (1.00)
PVK/PDOF(90/10)	3.12×10^{15} (1.41)	67.2 (1.07)	0.12 (0.33)	93.7 (1.35)	10.2 (1.33)	0.011 (0.23)	6637 (0.25)
PVK/PDHFF(90/10)	3.39×10^{15} (1.53)	68.1 (1.08)	0.03 (0.08)	121.5 (1.76)	13.1 (1.72)	0.0025 (0.05)	1601 (0.06)

^a The R_0 is calculated from eq 2 based on the following assumptions; k^2 (2/3), Q_D (0.5), n (1.0). ^b The E_T is obtained from eqs 3 and 4. ^c The r is obtained from eq 3. ^d The L is the length of the fully extended-side chain of PDAF. It is calculated by using HyperChem. ^e The k_T is calculated from eq 1. ^f Parentheses are the relative ratios based on the values of PVK/PDHF (90/10).

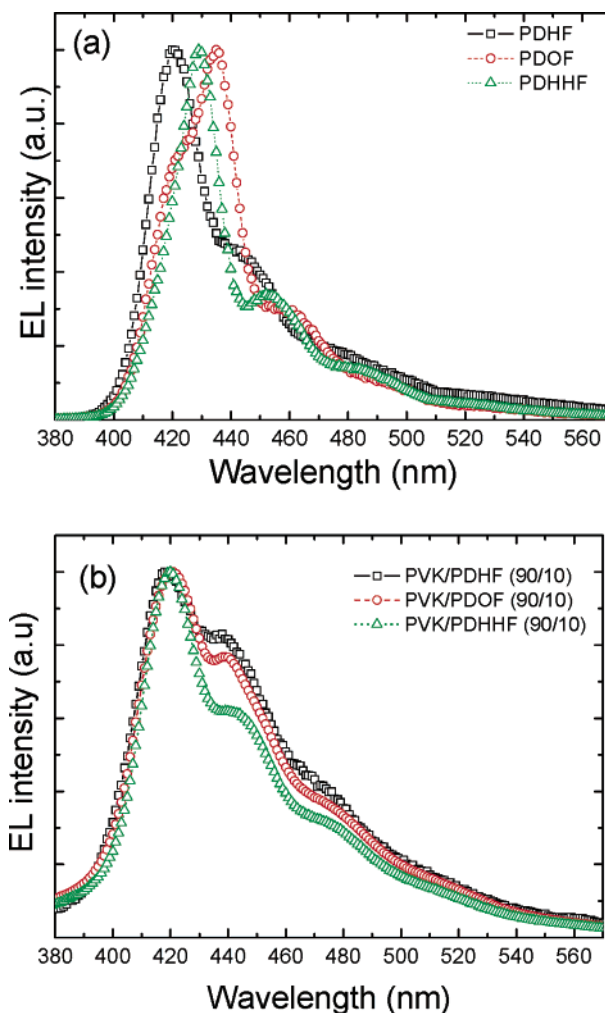
(r) is not a fixed value, but it may have different values of different blends.

The efficiency of energy transfer (E_T) is determined by the extent of donor quenching due to the acceptor⁴³ and obtained from Table 2 and eq 4 when it is assumed that the intensity decays of polymer blends are multi-exponential. The equation with a single exponential is also valid for the calculation of the efficiency (E_T).

$$E_T = 1 - \frac{\tau_{DA}}{\tau_D} \quad (4)$$

τ_D and τ_{DA} are fluorescence intensity decay times of donor in the absence and presence of acceptor as listed in Table 3. τ_D of PVK is assigned to 12.32 ns. τ_{DA} of PVK/PDHF, PVK/PDOF, and PVK/PDHFF are 7.87, 10.82, and 11.99 ns, which are calculated from the decay times above 1 ns. From eq 4, the efficiencies of energy transfer (E_T) of PVK/PDAF are 0.36 (PVK/PDHF), 0.12 (PVK/PDOF), and 0.03 (PVK/PDHFF). E_T of PVK/PDHFF is about 8% of PVK/PDHF. The donor–acceptor distances (r) of polymer blends could be obtained from eqs 3 and 4, but the calculated distances (70–121 Å) are somewhat large. We could suggest the reason in terms of the formation position of excitation energy in PVK and the side chain length of PDAF; the donor–acceptor distance (r) between PVK and PDAF may be obtained from their optically active chromophores. However, the probability of excimeric emission of PVK chromophores, which is formed from the localized sites of fully (or partially) eclipsed state of carbazole groups,⁴⁶ may be much smaller at the donor–acceptor interface than in PVK bulk. Most of the excitation energy in PVK is created in PVK bulk far from the blend interface. The side chain length of PDAF may also elucidate this large donor–acceptor distance (r). Therefore, the term r could be interpreted as the average separation distance between excitons of PVK and PDAF.

The fully extended-chain lengths of the substituents (L) and relative ratios are listed in Table 3. The relative ratios of the side chain lengths of PDOF and PDHFF to the side chain length of PDHF were calculated, which are 1.35 and 1.76. There are somewhat interesting results when L is compared to r in terms of energy transfer. When the relative ratios of the donor–acceptor distance (r) of PVK/PDOF and PVK/PDHFF to the donor–acceptor distance (r) of PVK/PDHF were calculated, their ratios are also 1.33 and 1.72. We calculated and compared the rates of energy transfer (k_T) in terms of the calculated donor–acceptor distance (r) and fully extended-chain length of polyfluorenes (L) by using eq 1. They are listed in Table 3. First, from the calculated donor–acceptor distance (r), the rate of energy transfer (k_T) of PVK/PDHF is 4.3 and 18.8 times larger than PVK/PDOF and PVK/PDHFF. Second, if the optically active chromophores of PVK are created much more at

**Figure 7.** EL spectra of (a) PDAF and (b) PVK/PDAF (90/10).

the interface as well as PVK bulk far from the interface, the donor–acceptor distance (r) could be a function of the side chain length of PDAF. With this assumption, we replaced the donor–acceptor distance (r) by the fully extended chain length (L) and calculated the rate of energy transfer (k_T) in eq 1, and the results are listed in Table 3. The rate of energy transfer (k_T) of PVK/PDHF is also 4.0 and 16.4 times larger than those of PVK/PDOF and PVK/PDHFF. The ratios of the rate of energy transfer calculated from the donor–acceptor distance (r) or the fully extended-chain length (L) are very similar. Therefore, the rate of energy transfer of PVK/PDHF is always 4–4.3 times and 16.4–18.8 times larger than PVK/PDOF and PVK/PDHFF regardless of the position of exciton formation in PVK. As alluded to above, the long and bulky side group (i.e., octyl, cyclohexylheptyl) of PDAF may fold the fluorene units much easier to reduce the dipole–dipole interactions and to

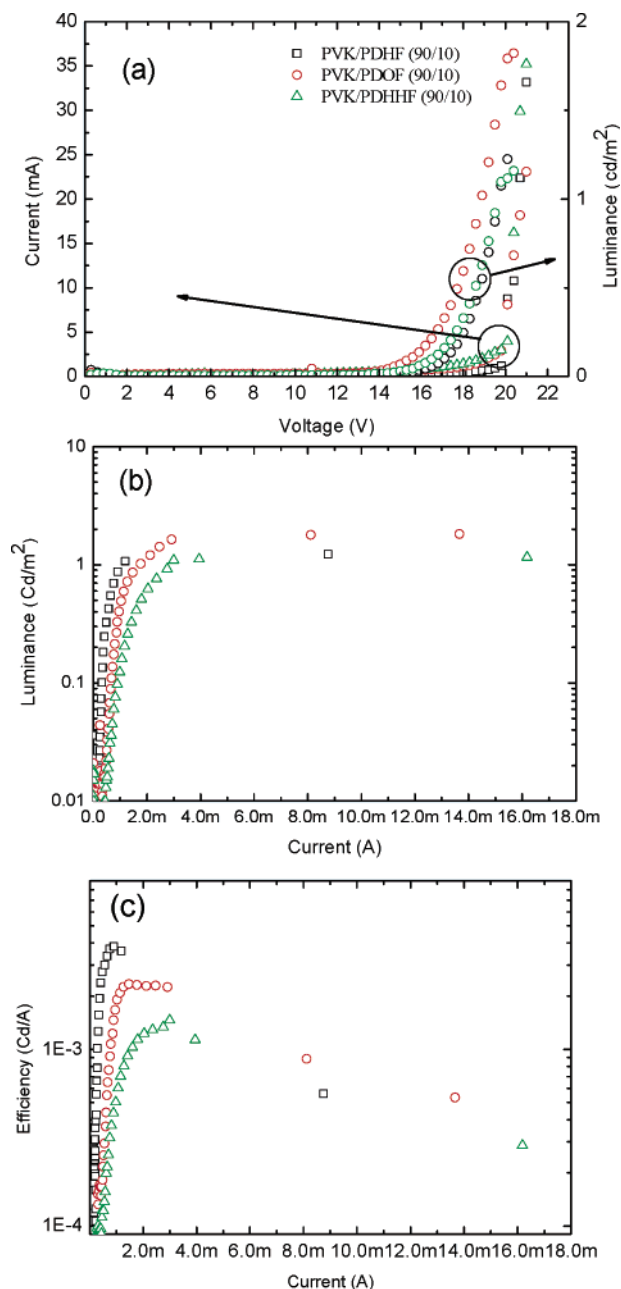


Figure 8. (a) Current–voltage–luminance, (b) luminance–current, and (c) efficiency–current of PVK/PDAF (90/10).

prevent the exciton energy formed in PVK from transferring to chromophores of PDAF. Finally, it could be concluded the side chain length and shape of PDAF affect the energy transfer process.

EL Properties of Polymer Blends. A PLED configuration with an ITO/PEDOT/light-emitting polymer/Al was fabricated to measure the EL properties. The EL spectra of PDAF and PVK/PDAF are shown in Figure 7. The EL peak wavelengths are 420 nm (PDHF), 435 nm (PDOF), and 429 nm (PDHFF). When 10 wt % of PDAF is blended with PVK, the EL emission wavelengths are about 420 nm. The current–voltage–luminance characteristics are shown in Figure 8a. Luminance–current relations are showed in Figure 8b. The current to get the brightness of 1 Cd/m² is 1.0 mA in the case of PVK/PDHF. It is the lowest among three blends because PVK/PDOF and PVK/PDHFF need 1.7 and 2.9 mA. In Figure 8c, the efficiencies of polymer blends are 3.82×10^{-3} Cd/A at 0.9 mA (PVK/PDHF),

2.34×10^{-3} Cd/A at 1.5 mA (PVK/PDOF), and 1.46×10^{-3} Cd/A at 3.0 mA (PVK/PDHFF). The efficiency of PVK/PDHF is 1.63 and 2.62 times larger than PVK/PDOF and PVK/PDHFF. Therefore, it could be suggested that the side chain length and shape of fluorene units may also affect the EL properties of polymer blends.

Conclusions

The side chains at the C-9 position of the fluorene in PDAF have the difference in length and shape. The effect of side chains on the PL of PVK/PDAF blends was investigated. 10 wt % content of PDAF is selected at which the blends show stronger PL intensity than the other blends with different contents. Excimeric emission in the polymer blends is suppressed due to acceptor dilution and energy transfer. PVK/PDHF (90/10) show the short donor–acceptor distance about 69 Å and the improved PL efficiency. However, PVK/PDHFF having long and bulky side chains shows the reduced efficiency of energy transfer, though its spectral overlap (J) is larger than the other blends, because the long and bulky side chains prevent the exciton formed at PVK from moving to PDAF. From time-resolved fluorescence intensity decay measurement, as the side chain lengths of fluorene decrease, the decay time of polymer blends also decrease, indicating the more efficient energy transfer occurs. The rate and the efficiency of energy transfer are dependent on the donor–acceptor distance which is affected by the side chain length of fluorene. Therefore, the side chain length and shape of fluorene affected the efficiency of energy transfer in PVK/PDAF blends.

Acknowledgment. We appreciate financial support from KOSEF (Korea Science and Engineering Foundation) and CAFPoly (Center for Advanced Functional Polymers). This work was also partially supported by the Brain Korea 21 program.

References and Notes

- (1) Friend, R. H.; Gymer, R. W.; Holmes, A. B.; Burroughes, J. H.; Marks, R. N.; Taliani, C.; Bradley, D. D. C.; Dos Santos, D. A.; Brédas, J. L.; Lögdlund, M.; Salaneck, W. R. *Nature (London)* **1999**, *397*, 121.
- (2) McGehee, M. D.; Heeger, A. J. *Adv. Mater.* **2000**, *12*, 1655.
- (3) Sariciftci, N. S. *Curr. Opin. Solid-State Mater. Sci.* **1999**, *4*, 373.
- (4) Chen, L.; McBranch, D. W.; Wang, H.; Helgeson, R.; Wudl, F.; Whitten, D. G. *Proc. Natl. Acad. Sci. U.S.A.* **1999**, *96*, 12287.
- (5) Sirringhaus, H.; Tessler, N.; Friend, R. H. *Science* **1998**, *280*, 1741.
- (6) Yu, G.; Wang, J.; McElvain, J.; Heeger, A. J. *Adv. Mater.* **1998**, *10*, 1431.
- (7) Ohmori, Y.; Uchida, M.; Muro, K.; Yoshino, K. *Jpn. J. Appl. Phys.* **1991**, *30*, L1941.
- (8) Fukuda, M.; Sawada, K.; Yoshino, K. *J. Polym. Sci., Polym. Chem.* **1993**, *31*, 2465.
- (9) Klaerner, G.; Lee, J. I.; Davey, M. H.; Miller, R. D. *Adv. Mater.* **1999**, *11*, 115.
- (10) Klaerner, G.; Miller, R. D. *Macromolecules* **1998**, *31*, 2007.
- (11) Gaal, M.; List, E. J. W.; Scherf, U. *Macromolecules* **2003**, *36*, 4236.
- (12) Scherf, U.; List, E. J. W. *Adv. Mater.* **2002**, *14*, 477.
- (13) Neher, D. *Macromol. Rapid Commun.* **2001**, *22*, 1365.
- (14) Iim, D. Y.; Cho, H. N.; Kim, C. Y. *Prog. Polym. Sci.* **2000**, *25*, 1089.
- (15) Moons, E. *J. Phys.: Condens. Matter* **2002**, *14*, 12235.
- (16) (a) Förster, T. *Ann. Phys.* **1948**, *2*, 55. (b) Rothberg, L. J.; Lovinger, A. J. *J. Mater. Res.* **1996**, *11*, 3174.
- (17) Byun, H. Y.; Chung, I. J.; Suh, Y.-S.; Shim, H. K.; Kim, D. Y.; Kim, C. Y. *Macromol. Symp.* **2003**, *192*, 151.
- (18) Nishino, H.; Yu, G.; Heeger, A. J.; Chen, T.-A.; Rieke, R. D. *Synth. Met.* **1995**, *68*, 243.

- (18) Mattoussi, H.; Murata, H.; Merritt, C. D.; Lizumi, Y.; Kido, J.; Kafafi, Z. H. *J. Appl. Phys.* **1999**, *86*, 2642.
- (19) Halls, J. J. M.; Cornil, J.; dos Santos, D. A.; Silbey, R.; Hwang, D.-H.; Holmes, A. B.; Brédas, J. L.; Friend, R. H. *Phys. Rev. B* **1999**, *60*, 5721.
- (20) Kulkarni, A. P.; Jenekhe, S. A. *Macromolecules*, **2003**, *36*, 5285.
- (21) Tang, H.-Z.; Fujiki, M.; Motonaga, M. *Polymer* **2002**, *43*, 6213.
- (22) Teetsov, J.; Fox, M. A. *J. Mater. Chem.* **1999**, *9*, 2117.
- (23) (a) Grell, M.; Bradley, D. D. C.; Ungar, G.; Hill, J.; Whitehead, K. S. *Macromolecules* **1999**, *32*, 5810. (b) Grell, M.; Bradley, D. D. C.; Inbasekaran, M.; Ungar, G.; Whitehead, K. S.; Woo, E. P. *Synth. Met.* **2000**, *579–581*, 111.
- (24) Winokur, M. J.; Slinker, J.; Huber, D. L. *Phys. Rev. B* **2003**, *67*, 184106.
- (25) Lieser, G.; Oda, M.; Miteva, T.; Meisel, A.; Nothofer, H. G.; Scherf, U.; Neher, D. *Macromolecules* **2000**, *33*, 4490.
- (26) (a) Kido, J.; Shionoya, H.; Nagai, K. *Appl. Phys. Lett.* **1995**, *67*, 2281. (b) Michelotti, F.; Borghese, F.; Bertolotti, M.; Ciani, E.; Foglietti, V. *Synth. Met.* **2000**, *105*, 111.
- (27) Kim, J. K.; Yu, J. W.; Cho, H. N.; Kim, D. Y.; Kim, C. Y. *Mol. Cryst. Liq. Cryst.* **1999**, *327*, 165.
- (28) Mort, J.; Pfister, G. *Electronic Properties of Polymers*; Wiley-Interscience: New York, 1982; pp 215–265.
- (29) Greczynski, G.; Kugler, Th.; Salaneck, W. R. *Thin Solid Films* **1999**, *354*, 129.
- (30) Marsitzky, D.; Murray, J.; Scott, J. C.; Carter, K. R. *Chem. Mater.* **2001**, *13*, 4285.
- (31) Suh, Y.-S.; Ko, S. W.; Jung, B.-J.; Shim, H.-K. *Opt. Mater.* **2002**, *21*, 109.
- (32) (a) Burroughes, J. H.; Bradley, D. D. C.; Brown, A. R.; Marks, R. N.; Mackay, K.; Friend, R. H.; Burns, P. L.; Holmes, A. B. *Nature (London)* **1990**, *347*, 539. (b) Carter, S. A.; Angelopoulos, M.; Karg, S.; Brock, P. J.; Scott, J. C. *Appl. Phys. Lett.* **1997**, *70*, 2067.
- (33) Meskers, S. C. J.; Hübner, J.; Oestreich, M.; Bäessler, H. *J. Phys. Chem. B* **2001**, *105*, 9139.
- (34) Jenekhe, S. A.; Osaheni, J. A. *Science* **1994**, *265*, 765.
- (35) Pei, Q.; Yang, Y. *J. Am. Chem. Soc.* **1996**, *118*, 7416.
- (36) Virgili, T.; Lidzey, D. G.; Bradley, D. D. C. *Adv. Mater.* **2000**, *12*, 58.
- (37) Conwell, E. *Synth. Met.* **1997**, *85*, 1.
- (38) Kim, J. L.; Cho, H. N.; Kim, J. K.; Hong, S. I. *Macromolecules* **1999**, *32*, 2065.
- (39) Alam, M. M.; Tonzola, C. J.; Jenekhe, S. A. *Macromolecules* **2003**, *36*, 6557.
- (40) Johnson, G. E. *J. Chem. Phys.* **1975**, *62*, 4697.
- (41) (a) Kersting, R.; Lemmer, U.; Mahrt, R. F.; Leo, K.; Kurz, H.; Bäessler, H.; Göbel, E. O. *Phys. Rev. Lett.* **1993**, *70*, 3820. (b) Lee, J.-I.; Kang, I.-N.; Hwang, D.-H.; Shim, H.-K. *Chem. Mater.* **1996**, *8*, 1925. (c) Cerullo, G.; Nisoli, M.; Stagira, S.; De Silvestri, S.; Lanzani, G.; Graupner, W.; List, E.; Leising, G. *Chem. Phys. Lett.* **1998**, *288*, 561. (d) Yu, J.-W.; Kim, J. K.; Cho, H. N.; Kim, D. Y.; Kim, C. Y.; Song, N. W.; Kim, D. *Macromolecules* **2000**, *33*, 5443. (e) Buckley, A. R.; Rahn, M. D.; Hill, J.; Cabanillas-Gonzalez, J.; Fox, A. M.; Bradley, D. D. C. *Chem. Phys. Lett.* **2001**, *339*, 331. (f) Meskers, S. C. J.; Hübner, J.; Oestreich, M.; Bäessler, H. *Chem. Phys. Lett.* **2001**, *339*, 223. (g) Dias, F. B.; Maçanita, A. L.; de Melo, J. S.; Burrows, H. D.; Güntner, R.; Scherf, U.; Monkman, A. P. *J. Chem. Phys.* **2003**, *118*, 7119.
- (42) Gupta, R.; Stevenson, M.; McGehee, M. D.; Dogariu, A.; Srdanov, V.; Park, J. Y.; Heeger, A. J. *Synth. Met.* **1999**, *102*, 875.
- (43) (a) Fung, B. K. K.; Stryer, L. *Biochemistry* **1978**, *17*, 5241. (b) Lakowicz, J. R. *Principles of Fluorescence Spectroscopy*, 2nd ed.; Kluwer Academic: Norwell, MA, 1999.
- (44) Haugland, R. P.; Yguerabide, J.; Stryer, L. *Proc. Natl. Acad. Sci. U.S.A.* **1969**, *63*, 23.
- (45) (a) Latt, S. A.; Cheung, H. T.; Blout, E. R. *J. Am. Chem. Soc.* **1965**, *87*, 996. (b) Gabor, G. *Biopolymers* **1968**, *6*, 809.
- (46) Roberts, A. J.; Cureton, C. G.; Philips, D. *Chem. Phys. Lett.* **1980**, *72*, 554.

MA04972W